Journal of Computational Analysis and Applications,Vol.7,No.3,319-349,2005,Copyright 2005 Eudoxus Press,LLC

Numerical Treatment Of The Two-dimensional Heat Radiation Integral Equation

Naji A. Qatanani* and Imad A. Barghouthi**

* Department of Mathematics, Al-Quds University, Jerusalem, Palestine.
nqatanani@science.alquds.edu

** Department of Physics, Al-Quds University, Jerusalem, Palestine.
barghouthi@yahoo.com

The radiation exchange in both convex and non-convex enclosures of diffuse gray surfaces is given in the form of a Fredholm boundary integral equation of the second kind. A boundary element method which is based on the Galerkin discretization schem is implemented for this integral equation. Four iterative methods are used to solve the linear system of equations resulted from the Galerkin discretization scheme. A comparison is drawn between these methods.
Theoretical error estimates for the Galerkin method has shown to be in a good agreement with numerical experiments.

KEYWORDS: Fredholm integral equation; heat radiation; iterative methods; error estimations.

1. INTRODUCTION

Transport of heat radiative energy between two points in convex or non-convex enclosures of diffuse gray surfaces is one of the few phenomena that are often governed directly by an integral equation. One of the consequences of this fact is that the pencil of rays emitted at one point can impinge another point only if these two points can "see" each other, i.e. the line segment connected these points does not intersect any surface. The presence of the shadow zones should be taken into account in heat radiation analysis whenever the domain where the radiation heat transfer is taking place, is not convex.

Shadow zones computation in some respect is not easy, but we were able to develop an efficient algorithm for this purpose and was implemented in our computer program. The integral equation governing the heat radiation (see section 2 for the formulation of the problem) was earlier solved for the convex enclosure using the Monte Carlo method [5].

In [2, 3] a boundary element method was implemented to obtain a direct numerical solution for this integral equation. This latter method permits quite high error bounds. For two-dimensional enclosure and three-dimensional rotational symmetric convex enclosure a Panel method has been developed [9] and then coupled with heat transport through radiation and conduction.

In this paper we are concerned to use the boundary element method, which is regarded to be the most popular numerical method for solving this type of problems. Thus we will present an efficient and reliable iterative methods to solve the linear system arises from Galerkin discretization scheme for the boundary integral equation. Numerical results for both convex and non-convex geometries have been obtained. We will present some error estimates for the Galerkin discretization method. Theoretically Galerkin method requires a time consuming double integral over Γ for the calculation of every element of the stiffness matrix. Thus we choose the corresponding numerical Gaussian quadrature formula with respect to a fast computation, i.e. by evaluating the kernel of the integral equation as seldom as possible. Numerical experiments with examples show high accuracy and efficiency of this method. The theoretical asymptotic error estimates are in rather good agreement with numerical experiments.

2. THE FORMULATION OF THE TWO DIMENSIONAL HEAT RADIATION PROBLEM

We consider an enclosure $\Omega \subset \mathbb{R}^2$ with boundary Γ. The boundary of the enclosure is composed of N elements as shown in Fig. 1.

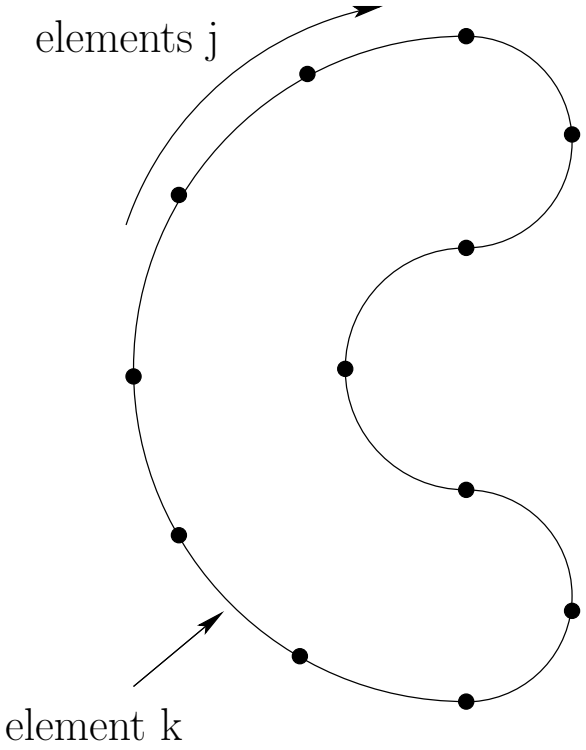

Fig.1

The heat balance for an element k with area dA_k reads as

$$Q_k = q_k dA_k = (q_{0,k} - q_{i,k}) dA_k, \tag{2.1}$$

where

$q_{i,k}$: is the rate of incomming radiant energy per unit area on the element k.
$q_{o,k}$: is the rate of outgoing radiant energy per unit area on the elment k.
dA_k : is the area of element k.
q_k : is the energy flux supplied to the element k by some means other than the radiation inside the enclosure to make up for the net radiation loss and maintain the specified inside surface temperature.

A second equation results from the fact that the energy flux leaving the surface is composed of emitted plus reflected energy. This yields to

$$q_{0,k} = \varepsilon_k \sigma T_4^k + l_k q_{i,k} \tag{2.2}$$

where

ε_k : is the emissivity coefficient $(0 < \varepsilon_k < 1)$.
σ : is the Stefan-Boltzmann constant which has the value $5.6696 \times 10^{-8}\ W/m^2K$.
l_k : is the reflection coefficient with the reation $l_k = 1 - \varepsilon_k$ is used for a gray surfaces.

The incident flux $q_{i,k}$ is composed of the portion of the energy leaving the viewable surfaces of the enclosure and arriving at the k-th surface. If the k-th surface can view itself (is non convex), a portion of its outgoing flux will contribute directly to its incidient flux. The incidient energy is then equal

$$\begin{aligned} dA_k q_{i,k} &= dA_1 q_{0,1} F_{1,k}\beta(1,k) + dA_2 q_{0,2} F_{2,k}\beta(2,k) + \ldots \\ &\quad + dA_j q_{0,j} F_{j,k}\beta(j,k) + \ldots + dA_k q_{0,k} F_{k,k}\beta(k,k) + \ldots \\ &\quad + dA_N q_{0,N} F_{N,k}\beta(N,k). \end{aligned} \tag{2.3}$$

From the view factor reciprocity relation [11] follows

$$\left.\begin{aligned} dA_1 F_{1,k}\beta(1,k) &= dA_k F_{k,1}\beta(k,1) \\ dA_2 F_{2,k}\beta(2,k) &= dA_k F_{k,2}\beta(k,2) \\ &\vdots \\ dA_N F_{N,k}\beta(N,k) &= dA_k F_{k,N}\beta(k,N) \end{aligned}\right\} \tag{2.4}$$

Then equation (2.3) can be rewritten in such a way that the only area appearing is dA_k:

$$\begin{aligned} dA_k q_{i,k} &= dA_k F_{k,1}\beta(k,1) q_{0,1} + dA_k F_{k,2}\beta(k,2) q_{0,2} + \ldots \\ &\quad + dA_k F_{k,j}\beta(k,j) q_{0,j} + \ldots + dA_k F_{k,k}\beta(k,k) q_{0,k} + \ldots \\ &\quad + dA_k F_{k,N}\beta(k,N) q_{0,N}. \end{aligned} \tag{2.5}$$

so that the incident flux can be expressed as

$$q_{i,k} = \sum_{j=1}^{N} F_{k,j}\beta(k,j) q_{0,j} \tag{2.6}$$

The visibility factor $\beta(k,j)$ is defined as (see for example [12])

$$\beta(k,j) = \begin{cases} 1 & \text{when there is a heat exchange between the} \\ & \text{surface element } k \text{ and the surface element } j \\ 0 & \text{otherwise} \end{cases} \tag{2.7}$$

Substituting (2.6) into (2.2) and using the relation $l_k = 1 - \varepsilon_k$ yields

$$q_{0,k} = \varepsilon_k \sigma T_k^4 + (1-\varepsilon_k) \sum_{j=1}^{N} F_{k,j} \beta(k,j) q_{0,j}. \tag{2.8}$$

2.1. The Calculation Of The View Factor $F_{k,j}$

The total energy per unit time leaving the surface element dA_k and incident at the element dA_j is given through

$$Q_{k,j} = L_k dA_k \cos(\theta_k) d\omega_k, \tag{2.9}$$

where $d\omega_k$ is the solid angle subtended by dA_j when viewed from dA_k (see Fig.2) and L_k is the total intensity of a black body leaving the element dA_k.

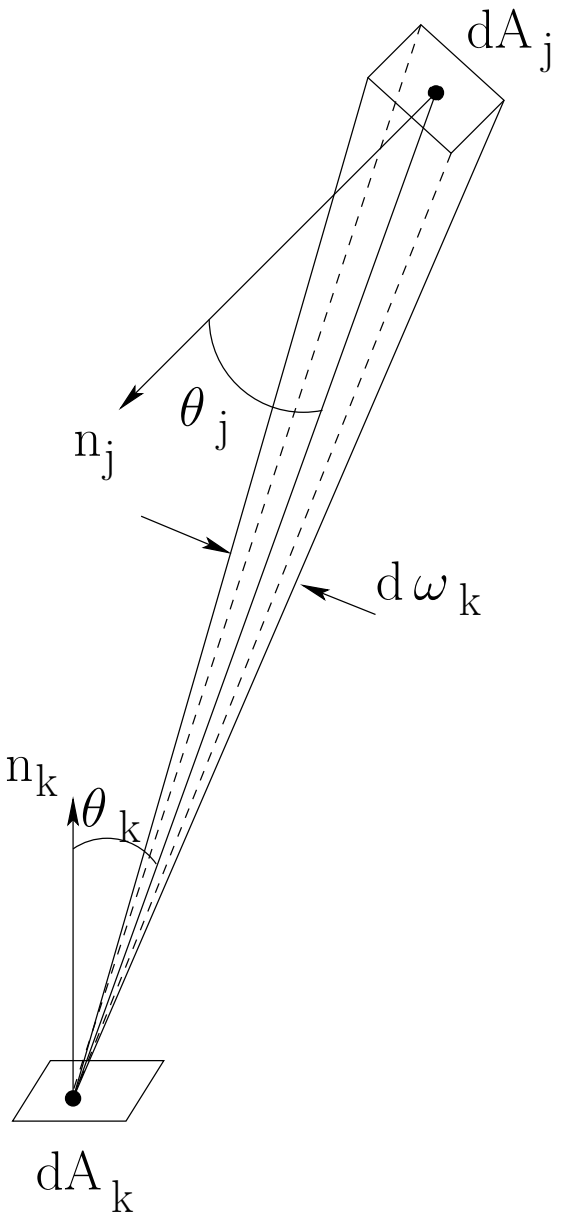

Fig.2

The solid angle $d\omega_k$ is related to the projected area dA_k and the distance $S_{k,j}$ between the elements dA_k and dA_j and can be calculated as

$$d\omega_k = \frac{dA_j \cos(\theta_j)}{S_{k,j}^2}, \tag{2.10}$$

where θ_j denotes the angle between the normal vector n_j and the distance vector $S_{k,j}$. Substituting (2.10) into (2.9) gives the following equation for the total energy per unit time leaving dA_k and arriving at dA_j:

$$Q_{k,j} = \frac{L_k dA_k \cos(\theta_k) dA_j \cos(\theta_j)}{S_{k,j}^2} \tag{2.11}$$

In [12], we have the relation between the total intensity E_k of a black body i.e.,

$$L_k = \frac{E_k}{\pi} = \frac{\sigma T_k^4}{\pi} \tag{2.12}$$

and consequantly equation (2.11) becomes

$$Q_{k,j} = \frac{\sigma T_k^4 \cos(\theta_k) \cos(\theta_j) dA_k dA_j}{\pi S_{k,j}^2}. \tag{2.13}$$

From the definition of the view factor $F_{k,j}$ (see [11]) together with (2.13), we get

$$F_{k,j} = \frac{Q_{k,j}}{\sigma T_k^4 dA_k} = \frac{\cos(\theta_k) \cos(\theta_j) dA_j}{\pi S_{k,j}^2}. \tag{2.14}$$

2.2. The Boundary Integral Equation

Now we are able to derive the boundary integral equation describing the heat balance in a gray body. The substitution of equation (2.14) into equation (2.8) leads to

$$q_{0,k} = \varepsilon_k \sigma T_k^4 + (1 - \varepsilon_k) \sum_{j=1}^{N} \frac{\cos(\theta_k) \cos(\theta_j) dA_j}{\pi S_{k,j}^2} \beta(k,j) q_{0,j}. \tag{2.15}$$

If the number of the area elements $N \to \infty$, then for all $x \in dA_k$ we obtain the following boundary integral equation

$$q_0(x) = \varepsilon(x) \sigma T^4(x) + (1 - \varepsilon(x)) \int_\Gamma G(x,y) q_0(y) d\Gamma_y \text{ for } x \in \Gamma, \tag{2.16}$$

where the kernel $G(x,y)$ denotes the view factor between the points x and y of Γ. From the above consideration and for general enclosure geometries $G(x,y)$ is given through

$$G(x,y) := G^*(x,y)\beta(x,y) = \frac{[n(y)\cdot(y-x)]\cdot[n(x)\cdot(x-y)]\cdot\beta(x,y)}{2|x-y|^3}. \qquad (2.17)$$

For convex enclosure geometries $\beta(x,y) \equiv 1$. If the enclosure ist not convex then we have to take into account the visibility function $\beta(x,y)$:

$$\beta(x,y) = \begin{cases} 1 & \text{for} \quad n(y)\cdot(y-x) \wedge n(x)\cdot(x-y) > 0 \wedge \vec{xy} \cap \Gamma = \emptyset \\ 0 & \text{for} \quad \vec{xy} \cap \Gamma \neq \emptyset \end{cases} \qquad (2.18)$$

where $\vec{xy}$ denotes the open straight segment between the points x and y. Definition (2.18) implies that $\beta(x,y) = \beta(y,x)$. Since $G^*(x,y)$ is symmetric then $G(x,y)$ is also symmetric.
Equation (2.16) is a Fredholm boundary integral equation of the second kind. We introduce the integral operator $\widetilde{K} : L^\infty(\Gamma) \to L^\infty(\Gamma)$ with

$$\widetilde{K}q_0(x) := \int_\Gamma G(x,y)q_0(y)d\Gamma_y \qquad \text{for } x \in \Gamma, q_0 \in L^\infty(\Gamma). \qquad (2.19)$$

Some of the properties of the integral operator (2.19) along with the solvability of equation (2.16) have been investigated in [12].

3. NUMERICAL APPROXIMATION TO THE SOLUTION OF THE FREDHOLM INTEGRAL EQUATION

3.1. Boundary Element Method and Galerkin Discretization

In a two-dimensional case we let Γ be a curve that is given by a regular parameter representation [10]

$$\Gamma : y = Z_j(t) \quad \text{for } t \in \mathbb{R},\ j = 1,\ldots,L \qquad (3.1)$$

We choose on $\mathbb{R}$ a family of 1-periodic interval partition:

$$0 = t_0 < t_< \cdots < t_N = 1,$$
$$\Pi_h = \{t_k\}_{-\infty}^{\infty},\ t_{k+N} = t_k + 1 \text{ with } h = max\{t_{k+1} - t_k\} \to 0. \qquad (3.2)$$

Let $S_h^{d,r}$ be a family of 1-periodic piecewise polynomials of degree $(d-1)$ with respect to the partition Π_h in the sense of Babuska an Aziz [1] which is $(r-1)$ times continuous and differntiable. We denote with $\Phi_k(t)$ the basis trial functions with a smallest possible support (B-splines) (see Fig.3).

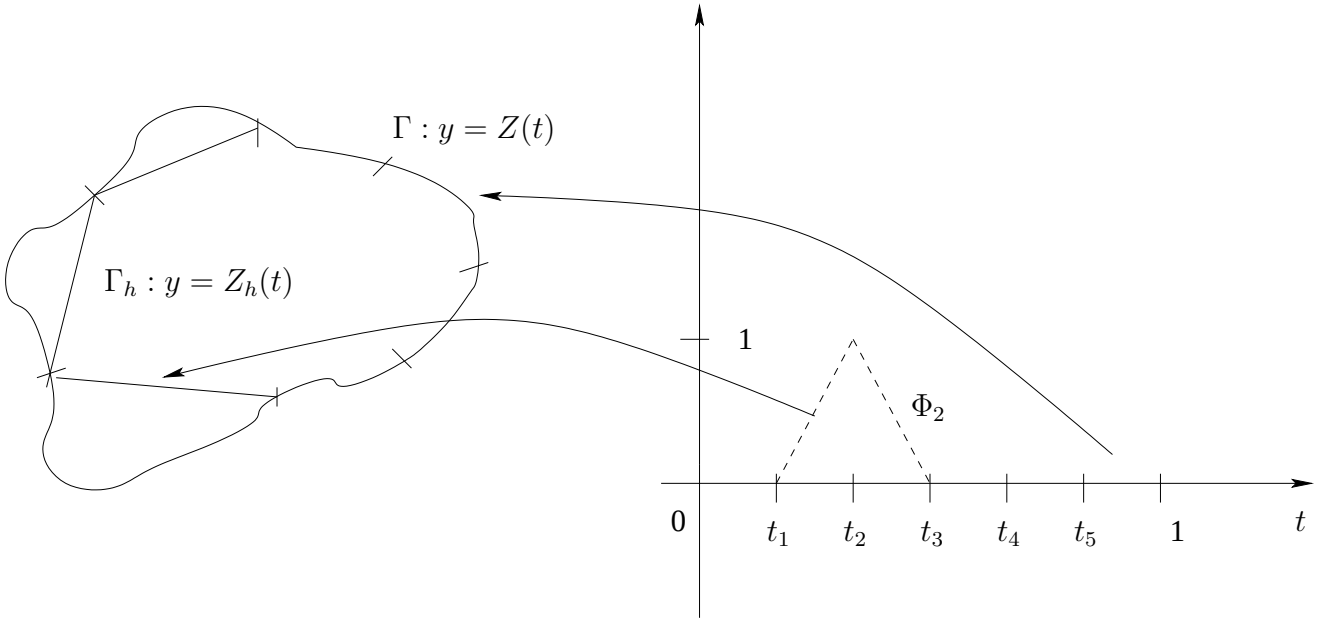

Fig. 3

The approximate solution has the general form

$$q_h(t) = \sum_{k=1}^{n} q_k \Phi_{k,n}(t) \qquad (3.3)$$

where n is the number of free grids and $q_k \in \mathbb{R}$, $k = 1, \ldots, n$ are the partition coefficients.

On partition in the parameter domain we use $S_h^{m+1,1}$-Lagrange-System of finite elements. Then the local representation of Γ transplant these finite element functions onto Γ_h. The ansatz functions (3.3) on Γ_h will then be defined by

$$\Gamma_h : y = Z_{jh}(t) \qquad (3.4)$$

with $Z_{jh}(t) = Z_j(t_k)$.
The ansatz functions (3.3) have the following approximation property

Approximation Property:
Let $\sigma \leq \tau \leq d$ be fulfilled and, for

$$\sigma < r + \frac{1}{2},\ \sigma < \frac{3}{2} \tag{3.5}$$

with the boundary approximation Γ_h, then there exists a constant c depending only on τ, σ and r and to any $v \in H^\tau(\Gamma)$ and any $S_h^{d,r}$ of our family there exists a finite element $\chi_h \in S_h^{d,r}$ such that

$$\|v - \chi_h\|_{H^\sigma(\Gamma)} \leq ch^{\tau-\sigma}\|v\|_{H^\tau(\Gamma)}. \tag{3.6}$$

Sometimes we shall additionally use the inverse property which holds for regular families $S_h^{d,r}$ subject to quasi-uniform of meshes.

Inverse Property:
For $\tau \leq \sigma$ with (3.5) there holds an estimate

$$\|\chi_h\|_{H^\sigma(\Gamma)} \leq c^* h^{\tau-\sigma}\|\chi_h\|_{H^\tau(\Gamma)} \quad \text{for } \chi_h \in S_h^{d,r} \tag{3.7}$$

where the constant c^* is independent of χ_h and h.

3.1.1. Representation Of System Of Equations

The Fredholm integral equation (2.16) can be expressed as

$$q = g + Kq \tag{3.8}$$

where $Kq = (1-\varepsilon)\widetilde{K}q$ and

$$\widetilde{K}q(x) = \int_\Gamma G(x,y)q(y)d\Gamma_y \quad \text{for } x \in \Gamma \text{ and } q \in L^\infty(\Gamma) \tag{3.9}$$

We let

$$\langle u, v\rangle_\Gamma := \int_0^1 u(t)v(t)|\dot{x}(t)|dt.$$

The Galerkin discretization of the integral equation (2.16) with the ansatz function (3.3) is given by

$$\sum_{k=1}^{n} q_k \langle \Phi_{k,n}, \Phi_{l,n} \rangle_\Gamma = \langle g, \Phi_{l,n} \rangle_\Gamma + \sum_{k=1}^{n} q_k \langle K\Phi_{k,n}, \Phi_{l,n} \rangle_\Gamma \tag{3.10}$$

Equation (3.10) can be written in the following short form:

$$(A_n - B_n)a_n = b_n \tag{3.11}$$

using the abbreviation $A = (q_{l,k})_{l,k=1,\ldots,n}$ for the mass matrix, with

$$q_{l,k} = \langle \Phi_{k,n}, \Phi_{l,n} \rangle_\Gamma = \int_0^1 \Phi_{l,n}(t)\Phi_{k,n}(t)|\dot{x}(t)|dt, \tag{3.12}$$

$B = (B_{l,k})_{l,k=1,\ldots,n}$ for the view factor matrix with

$$B_{l,k} = \langle K\Phi_{k,n}, \Phi_{l,n} \rangle_\Gamma = \int_0^1 \int_0^1 (1 - \varepsilon(t))\Phi_{l,n}(t)G(t,\tau)\Phi_{k,n}(\tau)|\dot{x}(t)||\dot{x}(\tau)|dtd\tau \tag{3.13}$$

and the vectors $a = (q_k)_{k=1,\ldots,n}$ and $b = \langle g, \Phi_{l,n} \rangle_\Gamma$, $l = 1, \ldots, n$.

Properties Of The Matrices

The mass matrix A in (3.11) is symmetric, positive definite and diagonal dominant hence it is invertible. Let λ_{min} and λ_{max} be the minimum and the maximum eigenvalues of the matrix A respectively then follows the well known estimations

$$\lambda_{min}\|q\|_{l^2}^2 \leq (A_n q, q) \leq \lambda_{max}\|q\|_{l^2}^2 \tag{3.14}$$

$$\frac{1}{\lambda_{max}}\|q\|_{l^2}^2 \leq (A_n^{-1} q, q) \leq \frac{1}{\lambda_{min}}\|q\|_{l^2}^2 \tag{3.15}$$

where $(\cdot,\cdot)$ denotes the Euclidean scalar product of $\mathbb{R}^n$ with $(q,q) = \|q\|_{l^2}^2$.

Furthermore holds

$$\|A_n\|_{l^2} = \lambda_{max}, \quad \frac{1}{\|A_n^{-1}\|_{l^2}} = \lambda_{min}. \tag{3.16}$$

Also the system of equations $(A_n - B_n)$ is symmetric and positve definite.
Since the mass matrix A is invertible, equation (3.11) can then be expressed in the form

$$(I - A_n^{-1}B_n)a_n = A_n^{-1}b_n \tag{3.17}$$

Equation (3.17) can also be written as

$$q_n = g_n + K_n q_n, \tag{3.18}$$

where $q_n = a_n, g_n = A_n^{-1}b_n$ and $K_n = A_n^{-1}B_n$.

3.1.2. Hiearchie Discretized Problem

The discretization parameter n defines in general the dimension of the problem. For the multi-grid method we use the hiearchie of discretization in multi levels. For each stepwise h_l there is a corresponding parameter n_l. Hence the discretized vector equation of level l has the form

$$q_{n_l} = g_{n_l} + K_{n_l} q_{n_l} \tag{3.19}$$

To avoid the double indices n_l, we use for short

$$q_l = g_l + K_l q_l \qquad (l \geq 0) \tag{3.20}$$

where $q_l = a_l, g_l = A_l^{-1}b_l$ and $K_l = A_l^{-1}B_l$.

3.2. Solution Methods

To solve equation (3.20) we use four approximate iterative methods. These are the Picard-iteration or Neumann series method, two-grid and multi-grid methods and the conjugate gradient method.

3.2.1. Picard-Iteration

This is one of the iterative approximate method in which the pre-iteration step

$$q_l^{i+1} = g_l + K_l q_l^i \tag{3.21}$$

with the iteration step index i is directly obtained from the linear system of equations. It converges if and only if the spectral radius

$$\rho(K_l) < 1 \tag{3.22}$$

holds [7].
A sufficient condition for the convergence of this iteration method is

$$\|K_l\| < 1 \tag{3.23}$$

for a suitable matrix norm.

3.2.2. Two-Grid Method

The usual two-grid iteration of level l for one iteration step $q_l^i \to q_l^{i+1}$:

Smoothing step: $$q_l^{i+1} = g_l + K_l q_l^i \quad i = 1, \ldots, \nu,\ \nu \geq 2 \tag{3.24}$$

Residues: $$r_l^{\nu+1} = (q_l^{\nu+1} - g_l - K_l q_l^{\nu+1}) \tag{3.25}$$

Breakdown criterion: $$\rho_l^{\nu+1} = \left\| r_l^{\nu+1} \right\|_2, \ \frac{\rho_l^{\nu+1}}{\rho_0} < \varepsilon \quad \text{stop}$$

Coarse grid correction: $$d_l = r(q_l^{\nu+1} - g_l - K_l q_l^{\nu+1}) \tag{3.26}$$

$$\delta_{l-1} = (I - K_{l-1})^{-1} d_{l-1} \tag{3.27}$$

$$q_{l+1}^0 = q_l^{\nu+1} - P\delta_{l-1} \tag{3.28}$$

Here r is $n_l \times n_{l-1}$ restriction matrix and P is $n_{l-1} \times n_l$ prolongation matrix. The indices $l-1$ and l are used for the coarse grid and fine grid respectively.

Convergence Of The Two-Grid Method

The mapping $q_l^i \to q_l^{i+1}$ of the two-grid algorithm is affined an has the representation

$$q_l^{i+1} = M_l^{TGM} q_l^i + C_l \tag{3.29}$$

where M_l^{TGM} is the two-grid iteration matrix.

Lemma 3.1. The two-grid iteration matrix M_l^{TGM} has the form [7]

$$M_l^{TGM} = \left[I - P(I - K_{l-1})^{-1} r(I - K_l)\right] K_l \quad \text{for all } l \geq 1$$

The partition of this matrix yields

$$\begin{aligned} M_l^{TGM} &= \left\{(I - Pr) + P(I - K_{l-1})^{-1}\left[(I - K_{l-1})r - r(I - K_l)\right]\right\} K_l \\ &= \left\{(I - Pr) + P(I - K_{l-1})^{-1}\left[rK_l - K_{l-1}r\right]\right\} K_l \end{aligned} \tag{3.30}$$

A sufficient condition for the convergence of this method ist the validity of the contraction condition

$$\left\|M_l^{TGM}\right\|_{A_l} < 1 \tag{3.31}$$

where M_l^{TGM} is given in (3.30).

3.2.3. Multi-Gird Method

The multi-grid iteration consists of a smoothing step and a coarse grid correction. The latter step uses the restricted defect $r(q_l^{\nu+1} - g_l - K_l q_l^{\nu+1})$. The resulting iteration is defined by the following recursive procedure:

Smoothing step: $$q_l^{i+1} = g_l + K_l q_l^i \quad i = 1, \ldots, \nu,\ \nu \geq 2 \tag{3.32}$$

Residues: $$r_l^{\nu+1} = (q_l^{\nu+1} - g_l - K_l q_l^{\nu+1}) \tag{3.33}$$

Breakdown criterion: $$\rho_l^{\nu+1} = \left\|r_l^{\nu+1}\right\|_2, \ \frac{\rho_l^{\nu+1}}{\rho_0} < \varepsilon \quad \text{stop}$$

Coarse grid correction: $$d_{l-1} = r(q_l^{\nu+1} - g_l - K_l q_l^{\nu+1}) \tag{3.34}$$

Multi-grid approximation $$(\delta_{l-1} = d_{l-1} + K_{l-1}\delta_{l-1}) \tag{3.35}$$

$$q_{l+1}^0 = q_l^{\nu+1} - P\delta_{l-1}. \tag{3.36}$$

Convergence Of The Multi-Grid Method

The mapping $q_l^i \to q_l^{i+1}$ of the multi-grid algorithm has the representation [7]

$$q_l^{i+1} = M_l^{MGM} q_l^i + C_l \tag{3.37}$$

where M_l^{MGM} is the multi-grid iteration matrix.

Lemma 3.2. The multi-grid iteration matrix M_l^{MGM} has the form [7]

$$M_l^{MGM} = M_l^{TGM} + P(M_{l-1}^{MGM})^2(I - K_{l-1})^{-1}r(I - K_l)K_l. \tag{3.38}$$

An alternative representation to (3.38) is

$$M_l^{MGM} = M_l^{TGM} + P(M_{l-1}^{MGM})^2\left[r - (I - K_{l-1})^{-1}(rK_l - K_{l-1}r)\right]K_l. \tag{3.39}$$

A sufficient condition for the convergence of this method ist the validity of the contraction condition

$$\left\|M_l^{MGM}\right\|_{A_l} < 1 \tag{3.40}$$

where M_l^{MGM} is given in (3.39).

3.2.4. Conjugate Gradient Iteration

This is an iteration method for solving the linear system

$$C_l a_l = b_l \tag{3.41}$$

where $C_l = (A_l - B_l)$.
It is an effective method for symmetric and positive definite systems.
This CG-iteration is given by the following algorithm [6]:

1. Choose an initial vector a_l^0 and compute $r_0 = C_l a_l^0 - b_l$.
   Set $p_0 = r_0$ and $k = 0$

2. Compute

$$\begin{aligned} \alpha_k &= \frac{r_k^T p_k}{p_k^T C_l p_k} \\ a_l^{k+1} &= a_l^k + \alpha_k p_k \\ r_{k+1} &= C_l a_l^{k+1} \end{aligned}$$

3. Stop if $\dfrac{\|r_{k+1}\|_2}{\|r_k\|_2} < \varepsilon$

4. Compute

$$\begin{aligned} \beta_k &= \frac{r_{k+1}^T C_l p_k}{p_k^T C_l p_k} \\ p_{k+1} &= r_{k+1} + \beta_l p_k. \end{aligned}$$

Convergence Of The Conjugate Gradient Method

From [12] follows that

$$\varepsilon \cdot \langle q, q \rangle_{L^2(\Gamma)} \leq \langle Aq, q \rangle_{L^2(\Gamma)} \leq (2 - \varepsilon) \cdot \langle q, q \rangle_{L^2(\Gamma)} \tag{3.42}$$

where $A = (I - K)$.
Let $q \in H_l \subset L^2(\Gamma)$ then we define

$$q(t) = \sum_{k=1}^{n_l} q_k \Phi_k(t). \tag{3.43}$$

Set equation (3.43) into (3.42) we get

$$\varepsilon \cdot \left\| \sum_{k=1}^{n_l} q_k \Phi_k \right\|_{L^2(\Gamma)}^2 \leq \sum_{k,j}^{n_l} q_k q_j \langle A\Phi_k, \Phi_j \rangle_{L^2(\Gamma)} \leq (2 - \varepsilon) \cdot \left\| \sum_{k=1}^{n_l} q_k \Phi_k \right\|_{L^2(\Gamma)}^2 . \tag{3.44}$$

Now

$$\left\| \sum_{k=1}^{n_l} q_k \Phi_k \right\|_{L^2(\Gamma)}^2 = \int_0^1 \left| \sum_{k=1}^{n_l} q_k \Phi_k(t) \right|^2 dt = \sum_{k,j}^{n_l} q_k q_j \int_0^1 \Phi_k(t) \Phi_j(t) dt = (A_l q, q) \tag{3.45}$$

Substituting (3.45) into (3.44) yields

$$\varepsilon (A_l q, q) \leq (C_l q, q) \leq (2 - \varepsilon) \cdot (A_l q, q). \tag{3.46}$$

Lemma 3.3. Let λ_k be the real, positive eigenvalue of the mass matrix A_l, and it holds

$$\left| \frac{\lambda_{max}}{\lambda_{min}} \right| \leq c \tag{3.47}$$

then follows

$$\lambda_{min}(q, q)_{A_l} \leq (A_l q, q) \leq \lambda_{max}(q, q)_{A_l}. \tag{3.48}$$

Thus one obtains

$$\lambda_{min}\|q\|^2_{l^2(\Gamma)} \leq (A_l q, q) \leq \lambda_{max}\|q\|^2_{l^2(\Gamma)}. \tag{3.49}$$

From (3.46) follows immediately

$$(\varepsilon)\lambda_{min}\|q\|^2_{l^2(\Gamma)} \leq (C_l q, q)_{A_l} \leq (2-\varepsilon)\cdot\lambda_{max}\|q\|^2_{l^2(\Gamma)}. \tag{3.50}$$

The condition number $\kappa(C_l)$ of the matrix C_l can then be estimated to give

$$\kappa(C_l) \leq \frac{(2-\varepsilon)\cdot\lambda_{max}}{(\varepsilon)\cdot\lambda_{min}} \tag{3.51}$$

using (3.47) then follows

$$\kappa(C_l) \leq c\cdot\frac{(2-\varepsilon)}{(\varepsilon)}\ .$$

Theorem 3.1. For a positive matrix C_l converges the Conjugate Gradient iteration with the convergence estimation [8]

$$\left\|e^k\right\|_{C_l} \leq 2\left(\frac{(\kappa(C_l)-1)^{\frac{1}{2}}}{(\kappa(C_l)+1)^{\frac{1}{2}}}\right)^k \left\|e^0\right\|_{C_l} \tag{3.52}$$

where $\left\|e^k\right\|_{C_l} = \left\|a_l^k - a_l\right\|_{C_l}$ and $\left\|e^0\right\|_{C_l} = \left\|a_l^0 - a_l\right\|_{C_l}$.

3.3. Computation Of The Visibility Function $\beta(x, y)$

We illustrate in the following steps the method for which how the visibility function $\beta(x, y)$ can be computed (see Fig.4)

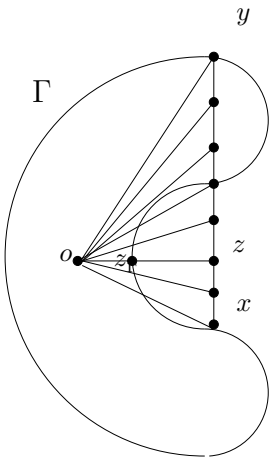

Fig.4

- We define

  G : be the straight segment between the points x and y

  $G := \{z \in \mathbb{R}^2 : z = x + \varphi(x + y), \varphi \in [0, 1]\}$.

  Question (1): is $G \subset \Omega$?

- We define

  $\widetilde{G}$: be the set of points such that

  $\widetilde{G} := \left\{z_i : z_i = x + \varphi_i \cdot (y - x), \varphi_i = \frac{i-1}{|x-y|}, i = 1, \ldots, m, m \in \mathbb{N}\right\}$

  $\widetilde{G}$ is thus an approximation of the line G.

  Question (2): is $\widetilde{G} \subset \Omega$?

  For all $z \in \widetilde{G}$

- We require the point 0 to be always situated in the region Ω,

- We determine next z_Γ, and

- Prove then if $|z_\Gamma| < |z|$

If this is the case then follows immediately that $\beta(x, y) = 0$

Question (3): How can z_Γ be determined ?

First we set $z_\Gamma = \alpha z, \alpha \in \mathbb{R}$.

The determination of α is necessary, therefore we demand

- $z_\Gamma \in \Gamma$ (see Fig.5)

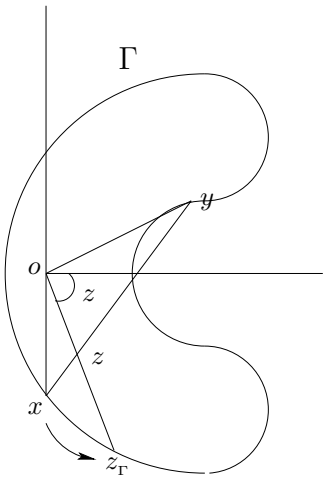

Fig.5

- $\arg z_\Gamma = \arg z$

To satisfy the first requirement, we set $x = X(t_0)$ and define $\Gamma = \{x = X(t), t \in [0,1]\}$. Determine next $t_1 = t_0 + \varepsilon$:
When $z_\Gamma = X(t_1)$, follows immediately the first requirement.

4. THE ASYMPTOTIC ERROR ANALYSIS

4.1. Theoretical Error Estimation

Most the asymptotic error estimates $\|q - q_h\|_{L^2(\Gamma)}$ are formulated in Sobolev spaces. It holds the following lemma

Lemma 4.1. (Cea's Lemma [10, 13])
The integral operator $A = I - K$ is a pseudodifferential operator of order zero. Therefore follows that for all $q \in L^2(\Gamma)$ the quasi-optimal error estimates

$$\|q - q_h\|_{L^2(\Gamma)} \leq c \inf_{w_h \in H_h} \|q - w_h\|_{L^2(\Gamma)} \tag{4.1}$$

holds, where the constant c is independent of h and q.

Theorem 4.1. The integral operator A is a strongly elliptic pseudodifferential operator of order α. Further holds for the two dimensional case

$$\alpha < 2r + 1 \tag{4.2}$$

Let $\alpha - d \leq \sigma \leq \frac{\alpha}{2} \leq \tau \leq d$ be satisfied and in addition let q_h be the Galerkin solution of the Galerkin equation

$$\langle Aq_h, w_h \rangle_{L^2(\Gamma)} = \langle g, w_h \rangle_{L^2(\Gamma)} \qquad \text{for all } w_h \in H_h$$

then we have the asymptotic error estimate

$$\|q_h - q\|_{H^\sigma(\Gamma)} \leq ch^{\tau-\sigma} \|q\|_{H^\tau(\Gamma)} \ . \tag{4.3}$$

Lemma 4.2. Let the ansatz functions be piecewise linear. Moreover $(I - K)$ is a pseudodifferential operator of order $\alpha = 0$, then follows from (4.3) the error estimate

$$\|q_h - q\|_{L^2(\Gamma)} \leq ch^2 \|q\|_{H^2(\Gamma)} . \tag{4.4}$$

For the boundary method one needs to compute numerically the coefficients $B_{l,k}$ of the view factor matrix B. Its computation is carried out by a suitable form of numerical integration. If the numerical integration is not accurately carried out then one expects quite high integration error. The accuracy of the numerical integration must be discussed in relation to the asymptotic error estimation therefore it is necessary to consider the following Lemma from Strang [4].

Theorem 4.2. (Strang Lemma [4])
We consider a family of approximated bilinear forms a_h which are uniformly H_h-elliptic. Then there exists a constant c that is independent of q and h and it holds the following inequality

$$\begin{aligned} \|q - q_h\|_{L^2(\Gamma)} \ \leq \ & c \left(\inf_{w_h \in H_h} \left\{ \|q - w_h\|_{L^2(\Gamma)} + \sup_{w_h \in H_h} \frac{|a(v_h, w_h) - a_h(v_h, w_h)|}{\|w_h\|_{L^2(\Gamma)}} \right\} \right. \\ & \left. + \sup_{w_h \in H_h} \frac{|g(w_h) - g_h(w_h)|}{\|w_h\|_{L^2(\Gamma)}} \right) \end{aligned} \tag{4.5}$$

where the terms $a(v_h, w_h)$, $g(w_h)$, $g_h(w_h)$ and $a_h(v_h, w_h)$ in (4.5) are defined as follows

$a(v_h, w_h) = \langle (I-K)v_h, w_h \rangle_{L^2(\Gamma)} = \langle Av_h, w_h \rangle_{L^2(\Gamma)}$

$g(w_h) = \langle g, w_h \rangle_{L^2(\Gamma)}$

$g_h(w_h) = \langle g_h, w_h \rangle_{L^2(\Gamma)}$

and

$a_h(v_h, w_h) = \langle a_h, w_h \rangle_{L^2(\Gamma)}$.

The approximation $a_h(v_h, w_h)$ has the form

$$\begin{aligned} a_h(v_h, w_h) &= \int_\Gamma (I-K)v_h w_h d\Gamma_x = \int_\Gamma v_h(x) w_h(x) d\Gamma_x \\ &\quad - \int_\Gamma \int_\Gamma (1-\varepsilon(x)) G(x,y) v_h(x) w_h(y) d\Gamma_x d\Gamma_y \end{aligned}$$

The coefficients $A_{k,l}$ of the mass matrix A (without the Quadrature error) are

$$A_{k,l} = a(\Phi_k, \Phi_l) = \sum_{k=1}^{n} \left\{ \int_\Gamma \Phi_k(x)\Phi_l(x) d\Gamma_x - \int_\Gamma \int_\Gamma (1-\varepsilon(x)) G(x,y) \Phi_k(x) \Phi_l(y) d\Gamma_x d\Gamma_y \right\}.$$

If we now replace the above integration by Gaussian quadrature. This yields the following approximation formula

$$\widetilde{A}_{k,l} = a_h(\Phi_k, \Phi_l) = \sum_{i=1}^{m} W_i F_{k,l}(x_i) + \sum_{i=1}^{m} \sum_{j=1}^{m} W_i W_j E_{k,l}(x_i, y_j),$$

where $F_{k,l}$ and $E_{k,l}$ are given by

$$F_{k,l} = \Phi_k(x)\Phi_l(x),$$

and

$$E_{k,l}(x,y) = (1-\varepsilon(x)) G(x,y) \Phi_k(x) \Phi_l(y)$$

here m denotes the order of the quadrature and the coefficients W_i and W_j are the weights of the quadrature form.

The ellipticity of a_h follows directly from Lemma 2.8 [12].

It holds

$$\varepsilon \|q\|^2_{L^2(\Gamma)} \leq \langle Aq, q \rangle_{L^2(\Gamma)} \leq (2-\varepsilon) \|q\|^2_{L^2(\Gamma)} \tag{4.6}$$

Let the approximation operator A_h satisfies the approximation inequality

$$\|(A - A_h)q\|_{L^2(\Gamma)} \leq c h_l^\tau \|q\|_{H^\tau(\Gamma)} \tag{4.7}$$

where τ is defined in (3.5).
Let q_h be our assigned ansatz function, then follows

$$\varepsilon\|q_h\|^2_{L^2(\Gamma)} \leq \langle Aq_h, q_h\rangle_{L^2(\Gamma)} + ch_l^{\tau}\|q_h\|_{H^{\tau}(\Gamma)} \cdot \|q_h\|_{L^2(\Gamma)} \tag{4.8}$$

with the help of the inverse inequality (3.7) we get

$$\varepsilon\|q_h\|^2_{L^2(\Gamma)} \leq \langle Aq_h, q_h\rangle_{L^2(\Gamma)} + c_1^* \left(\frac{h_l}{h_{l-1}}\right)^{\tau} \|q_h\|^2_{L^2(\Gamma)}. \tag{4.9}$$

Finally we obtain

$$\left(\varepsilon - c_1^* \left(\frac{h_l}{h_{l-1}}\right)^{\tau}\right) \|q_h\|^2_{L^2(\Gamma)} \leq \langle A_h q_h, q_h\rangle_{L^2(\Gamma)} \tag{4.10}$$

under the assumption $c_2^* \leq \left(\frac{h_l}{h_{l-1}}\right) \leq c_3^*$ one obtains for the case $\tau = 1$

$$\langle A_h q_h, q_h\rangle_{L^2(\Gamma)} \geq \frac{1}{2}\varepsilon \cdot \|q_h\|^2_{L^2(\Gamma)}. \tag{4.11}$$

Hence ellipticity is proved. From this condition follows how exact the numerical quadrature error must be.

5. NUMERICAL RESULTS

5.1. Numerical Examples For The Solution Of The System Of Equations

Since the convergence requirements of the four solution methods are satisfied [12], then we can apply now these methods to solve the following two-dimensional convex and non-convex enclosures.

Convex Enclosure

Example 5.1. Let Ω be the domain of an ellipse. The boundary of this ellipse has the following parameterization

$$Gamma = \left\{ x \in \mathbb{R}^2 : x = \begin{pmatrix} a\cos 2\pi t \\ b\sin 2\pi t \end{pmatrix}, a = 4, b = 2, 0 \leq t < 1 \right\}. \tag{5.1}$$

The computation of the coefficients $A_{l,k} = \langle \Phi_{k,n}, \Phi_{l,n} \rangle$, $b_n = \langle g, \Phi_{l,n} \rangle$ and $B_{l,k} = \langle K\Phi_{k,n}, \Phi_{l,n} \rangle$ have been carried out be Gaussian quadrature form.
Here we have $g(t) = \varepsilon(t)\sigma T^4(t)$ with
The emissivity coefficient $\varepsilon = 0.9$
The Boltzmann coefficient $\sigma = 5.6696 \times 10^{-8}$ and
The surface temperature $T(t) = \frac{1}{2}(T_1 + T_2) - \frac{1}{2}(T_2 - T_1)\cos 2\pi t$, where $T_1 = 1000$ and $T_2 = 1800$.
Table (I) shows the numerical results for the solutions of equation (3.20) by using Picard's iteration, two-grid and multi-grid methods and CG-iteration method for the ellipse. It contains both the number of iteration steps and the required CPU-time in second. The mesh width $h_l = \frac{1}{n_l}$ with $n_l = 2^l$. The number $n = n_l$ denotes the parameter of the solved problem. The four iteration methods converge for all levels l. Comparing these iterations together we see clearly that the two-grid and multi-grid methods require both a small number of iterations and CPU-time in comparison with the Picard's iteration. On the other hand the CG-iteration needs more iteration steps but less CPU-time in comparison with the other methods.

Table I. Solution Methods for an Ellipse

n_l	Picard		Two-grid		Multi-grid		CG	
	Iter	sec	Iter	sec	Iter	sec	Iter	sec
32	14	< 1	6	< 1	2	< 1	16	< 1
64	14	0.50	6	< 1	2	< 1	18	< 1
128	14	2.02	6	1.12	2	< 1	19	< 1
256	14	8.05	6	4.42	2	1.51	20	0.51
512	14	32.09	6	16.69	2	6.01	20	2.05
1024	14	128.26	6	69.98	2	24.07	20	8.16

Non-Convex Enclosure

Example 5.2. We consider for an example the non-convex curve shown in Fig.6. In this case the visibility function $\beta(t, \tau)$ must be taken into consideration, with $\beta(t, \tau)$ is defined in (2.18). The computation of this visibility function has been

illustrated in section 3.3. Table (II) contains the numerical resuts for this non-convex case.

Table II. Solution Methods for the Nonconvex Curve in Fig.6

n_l	Picard		Two-grid		Multi-grid		CG	
	Iter	sec	Iter	sec	Iter	sec	Iter	sec
32	16	< 1	8	< 1	3	< 1	27	< 1
64	16	0.58	8	< 1	3	< 1	31	< 1
128	16	2.31	8	1.38	3	0.53	40	< 1
256	16	9.14	8	5.49	3	2.09	43	1.07
512	16	36.50	8	21.98	3	8.31	43	4.23
1024	16	145.48	8	86.92	3	33.02	43	16.88

5.2. Numerical Examples For The Error Estimation

5.2.1. Convex Case

a) Γ Describes the boundary of a circle

Example 5.3. Let $q(t) = \cos 2\pi t$ for $0 \le t \le 1$ be the exact solution of the integral equation

$$q(t) = g(t) + (1 - \varepsilon) \int_0^1 G^*(t, \tau) q(\tau) |\dot{x}(\tau)| d\tau \ . \tag{5.2}$$

Then the exact $g(t)$ for the given exact $q(t)$ has been calculated as follows
For the unit circle $\vec{n}(\tau) \cdot (\vec{t} - \vec{\tau}) = \frac{1}{2}$ and $|\vec{\tau} - \vec{t}| = 2|\sin \pi(t - \tau)|$.
Then the kernel $G^*(t, \tau)$ in (2.17) reduced to

$$G^*(t, \tau) = \frac{1}{2} \cdot \frac{1}{4} |\vec{t} - \vec{\tau}| = \frac{1}{4} |\sin \pi(t - \tau)|. \tag{5.3}$$

Substituting (5.3) into (5.2) with $|\dot{x}(\tau)| = \cos 2\pi t$ to obtain the exact $g(t)$ as

$$g(t) = \cos 2\pi t + \frac{1}{3}(1 - \varepsilon(t)) \cos 2\pi t \tag{5.4}$$

This computed exact $g(t)$ in (5.4) has then been used in our program to obtain the approximat solution q_h with the help of our numerical iterations.

b) Γ Describes the boundary of square

Example 5.4. Let $q(t) = x_1(t)$ be the exact solution for the case of a unit square. Then the exact $g(t)$ can be computed as follows:
For $t \geq 0$ and $t < 0.25$ we have

$$\begin{aligned} g_1(t) &= 4t - 4(1-\varepsilon(t)) \left\{ \int_0^{1/4} G_{11}^*(t-\tau)\cdot 4\tau d\tau + \int_{1/4}^{1/2} G_{12}^*(t,\tau)\cdot 1 d\tau \right. \\ &\quad \left. + \int_{1/2}^{3/4} G_{13}^*(t-\tau)\cdot(3-4\tau)d\tau + \int_{3/4}^{1} G_{14}^*(t,\tau)\cdot 0 d\tau \right\}, \end{aligned} \tag{5.5}$$

where
$G_{11}^* = 0, \qquad G_{12}^* = G_{21}^* = \dfrac{(1-4t)(4\tau-1)}{2\left[(4t-1)^2+(4\tau-1)^2\right]^{2/3}},$
$G_{13}^* = G_{31}^* = \dfrac{1}{2\left[16(t-\frac{3}{4}+\tau)^2+1\right]^{2/3}}$ and
$G_{14}^* = G_{41}^* = \dfrac{16t}{2\left[16t^2+16(1-\tau)^2+1\right]^{2/3}}$

For $t \geq 0.25$ and $t < 0.5$ we have

$$\begin{aligned} g_2(t) &= 1.0 - 4(1-\varepsilon(t)) \left\{ \int_0^{1/4} G_{21}^*(t,\tau)\cdot 4 d\tau + \int_{1/4}^{1/2} G_{22}^*(t,\tau)\cdot 1 d\tau \right. \\ &\quad \left. + \int_{1/2}^{3/4} G_{23}^*(t,\tau)\cdot(3-4\tau)d\tau + \int_{3/4}^{1} G_{24}^*(t,\tau)\cdot 0 d\tau \right\}, \end{aligned} \tag{5.6}$$

with $G_{22}^* = 0, \qquad G_{23}^* = G_{32}^* = \dfrac{(1-2t)(2\tau-1)}{2\left[(2t-1)^2+(2\tau-1)^2\right]^{2/3}},$
and $G_{24}^* = G_{42}^* = \dfrac{1}{2\left[16(t-\frac{5}{4}+\tau)^2+1\right]^{2/3}}.$

For $t \geq 0.5$ and $t < 0.75$ we have

$$\begin{aligned} g_3(t) &= (3-4t) - 4(1-\varepsilon(t)) \left\{ \int_0^{1/4} G_{31}^*(t,\tau)\cdot 4\tau d\tau + \int_{1/4}^{1/2} G_{32}^*(t,\tau)\cdot 1 d\tau \right. \\ &\quad \left. + \int_{1/2}^{3/4} G_{33}^*(t,\tau)\cdot(3-4\tau)d\tau + \int_{3/4}^{1} G_{34}^*(t,\tau)\cdot 0 d\tau \right\}, \end{aligned} \tag{5.7}$$

where $G^*_{33} = 0$ and $G^*_{34} = G^*_{43} = \dfrac{(3-4t)(4\tau-3)}{2\left[(3-4t)^2+(4\tau-3)^2\right]^{2/3}}$.

For $t \geq 0.75$ and $t < 1.0$ holds

$$g_4(t) = -4(1-\varepsilon(t))\left\{\int_0^{1/4} G^*_{41}(t,\tau)\cdot 4\tau d\tau + \int_{1/4}^{1/2} G^*_{42}(t,\tau)\cdot 1 d\tau + \int_{1/2}^{3/4} G^*_{43}(t,\tau)\cdot(3-4\tau)d\tau + \int_{3/4}^{1} G^*_{44}(t,\tau)\cdot 0 d\tau\right\}, \qquad (5.8)$$

where $G^*_{44} = 0$.

The exact $g(t)$ in (5.5), (5.6), (5.7) and (5.8) has been explicity calculated. Tables (III) and (IV) contain the numerical results for the two computed $g(t)$ in (5.4) and (5.5 − 5.8) respectively. They show the L_2-error $\|q-q_h\|_{L^2}$ and the order of convergence. In this case we obtain an error estimation for $\|q-q_h\|_{L^2}$ of order $O(h^2)$.

We conlude that the theoretical error estimation (4.4) and the numerical results in tables (III) and (IV) are equivalent.

Table III. Error Estimation

Theoretical Value = 2.0

l	n_l	L_2-Error	Conv. Ord
2	4	8.505×10^{-2}	
3	8	1.747×10^{-2}	2.28
4	16	4.139×10^{-3}	2.08
5	32	1.021×10^{-3}	2.02
6	64	2.536×10^{-4}	2.01
7	128	6.534×10^{-5}	2.00
8	256	1.588×10^{-5}	2.00
9	512	3.976×10^{-6}	2.00

Table IV. Error Estimation

Theoretical Value = 2.0

l	n_l	L_2-Error	Conv. Ord
2	4	4.457×10^{-2}	
3	8	9.483×10^{-3}	2.23
4	16	2.207×10^{-3}	2.10
5	32	5.490×10^{-4}	2.01
6	64	1.369×10^{-4}	2.01
7	128	3.414×10^{-5}	2.00
8	256	5.537×10^{-6}	2.00
9	512	2.139×10^{-6}	2.00

5.2.2. Non-Convex Case

Example 5.5. Let

$$q(t) = 1 + \begin{cases} t^2(t-\frac{1}{4})^2 & \text{for } t \in [0, \frac{1}{4}) \\ (t-\frac{1}{4})^2(t-\frac{1}{2})^2 & \text{for } t \in [\frac{1}{4}, \frac{1}{2}) \\ (t-\frac{1}{2})^2(t-\frac{3}{4})^2 & \text{for } t \in [\frac{1}{2}, \frac{3}{4}) \\ (t-\frac{3}{4})^2(t-1)^2 & \text{for } t \in [\frac{3}{4}, 1) \end{cases} \tag{5.9}$$

be the exact solution for the non-convex curve (see Fig.6),

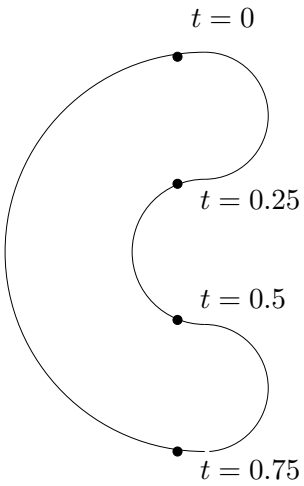

Fig.6

then the exact $g(t)$ can be calculated from the integral equation (2.17) as follows: For $t \geq 0$ and $t < 0.5$ we have

$$g_1(t) = q_1(t) - (1 - \varepsilon(t)) \left(\int_0^{1/4} G_1(t, \tau) \cdot q_1(\tau) \cdot 4\pi d\tau \right) \tag{5.10}$$

where $q_1(t) = 1 + t^2(t - \frac{1}{4})^2$ and $G_1(t, \tau) = \frac{1}{4} |\sin 2\pi(t - \tau)|$.

For $t \geq 0.25$ and $t < 0.5$ we have

$$g_2(t) = q_2(t) - (1 - \varepsilon(t)) \left(\int_{1/4}^{1/2} G_2(t, \tau) \cdot q_2(\tau) \cdot 4\pi d\tau \right) \tag{5.11}$$

where $q_2(t) = 1 + (t - \frac{1}{4})^2(t - \frac{1}{2})^2$ and $G_2(t, \tau) = \frac{1}{4} |\sin 2\pi(t - \tau)|$.

For $t \geq 0.5$ and $t < 0.75$ we have

$$g_3(t) = q_3(t) - (1 - \varepsilon(t)) \left(\int_{1/2}^{3/4} G_3(t, \tau) \cdot q_3(\tau) \cdot 4\pi d\tau \right) \tag{5.12}$$

where $q_3(t) = 1 + (t - \frac{1}{2})^2(t - \frac{3}{4})^2$ and $G_3(t, \tau) = \frac{1}{4} |\sin 2\pi(t - \tau)|$.

For $t \geq 0.75$ and $t < 1.0$ we have

$$g_4(t) = q_4(t) - (1 - \varepsilon(t)) \left(\int_{3/4}^{1} G_4(t, \tau) \cdot q_4(\tau) \cdot 12\pi d\tau \right) \tag{5.13}$$

where $q_4(t) = 1 + (t - \frac{3}{4})^2(t - 1)^2$ and $G_4(t, \tau) = \frac{1}{12} |\sin 2\pi(t - \tau)|$.

The exact $g(t)$ in (5.10), (5.11), (5.12) and (5.13) has been explicity computed. Table (V) contains the numerical results for this computed exact $g(t)$ (5.10 − 5.13). The table shows the L_2-error $\|q - q_h\|_{L^2}$ and the order of convergence. We see clearly that the L_2-error $\|q - q_h\|_{L^2}$ for this non-convex case is of order $O(h^2)$. We finally conclude that the theoretical error estimation (4.4) for $\|q - q_h\|_{L^2}$ and the numerical results in table (V) for the non-convex case are in good agreement.

Table V. Error Estimation

Theoretical Value = 2.0

l	n_l	L_2-Error	Conv. Ord
2	4	1.2345×10^{-1}	
3	8	2.6834×10^{-2}	2.16
4	16	6.3138×10^{-3}	2.09
5	32	1.5437×10^{-3}	2.03
6	64	3.8210×10^{-4}	2.01
7	128	9.5049×10^{-5}	2.01
8	256	2.3760×10^{-5}	2.00
9	512	5.9400×10^{-6}	2.00

REFERENCES

[1] I. Babuska and A.K. Aziz: Survey Lectures on the mathematical foundations of the Finite Element Method. In: The Mathematical Foundations of the Finite Element Method with Applications to Partial Differential Equations. A.K. Aziz (ed.) Academic Press, New York-London (1972).

[2] R.A. Bialecki, Boundary element calculation of the radiative heat sources. In: Advanced Comp. Methods in Heat Transfer II Vol. 1 (I.C. Wrobel, C.A. Brebbia, A. J. Nowak eds) Elsevier, London (1992).

[3] R.A. Bialecki, Solving Heat Radiation Problems Using the Boundary Element Method. Computational Mechanics Publications, Hobbs Ltd., Southampton (1993).

[4] P.G. Ciarlet, The Finite Element Methods For elliptic Problems. North-Holland Publishing Company, Amsterdam-New York-Oxford (1980).

[5] M.F. Cohen and J.R. Wallace, Radiosity and Realistic Image Synthesis. Academic Press, New York-London (1993).

[6] W. Hackbusch, Multi-Grid Methods and Applications. Springer Verlag, Berlin-New York (1985).

[7] W. Hackbusch, Integralgleichungen. Theorie und Numerik. B.G. Teubner, Stuttgart (1989).

[8] M. Hestens and E. Stiefel, Methods of conjugate gradients for solving linear systems. J. Respectively. Nat. Bur. Stand. **49** (1952) 409-436.

[9] C. Rihaczek, Anwendung Objektorientierter Techniken zur Berechnung des Gekoppelten Wärmetransports durch Leitung und Strahlung. Doktorarbeit 1993, Universität Stuttgart.

[10] A.H. Schatz, V. Thomee and W.L. Wendland, Mathematical Theory of Finite and Boundary Element Methods. Birkhaeuser Verlag, Basel-Boston-Berlin (1990).

[11] R. Siegel and J.R. Howell, Thermal Radiation Heat Tansfer. Hemisphere Publishing Corp., New York (1981).

[12] N. Qatanani, Lösungsverfahren und Analysis der Integralgleichung für das Hohlraum-Strahlungs-Problem. Doktorarbeit 1996, Universität Stuttgart.

[13] W.L. Wendland, Strong elliptic booundary integral equations. In: The State of the Art in Numerical Analysis. (eds. A. Iserles and M. Powell). Clarendon Press, Oxford (1987) 511-561.